Nuclear magnetic resonance and small-angle X-ray scattering studies of mixed sodium dodecyl sulfate and N,N-dimethyldodecylamine N-oxide aqueous systems performed at low temperatures

Summerton, Emily; Hollamby, Martin J.; Le Duff, Cécile S.; Thompson, Emma S.; Snow, Tim; Smith, Andrew J.; Jones, Christopher; Bettiol, Jeanluc; Bakalis, Serafim; Britton, Melanie M.

DOI:
10.1016/j.jcis.2018.09.053

Journal of Colloid and Interface Science 535 (2019) 1–7

Contents lists available at ScienceDirect

Journal of Colloid and Interface Science

journal homepage: www.elsevier.com/locate/jcis

Nuclear magnetic resonance and small-angle X-ray scattering studies of mixed sodium dodecyl sulfate and N,N-dimethyldodecylamine N-oxide aqueous systems performed at low temperatures

Emily Summerton [a], Martin J. Hollamby [b], Cécile S. Le Duff [c], Emma S. Thompson [c], Tim Snow [d], Andrew J. Smith [d], Christopher Jones [e], Jeanluc Bettiol [e], Serafim Bakalis [a], Melanie M. Britton [c,*]

[a] School of Chemical Engineering, University of Birmingham, Edgbaston, B15 2TT, UK
[b] School of Chemical and Physical Sciences, University of Keele, Keele ST5 5TG, UK
[c] School of Chemistry, University of Birmingham, Edgbaston, B15 2TT, UK
[d] Diamond Light Source, Harwell Science and Innovation Campus, Didcot OX11 0DE, UK
[e] Procter & Gamble Brussels Innovation Centre, Temselaan 100, 1853, Strombeek Bever, Belgium

GRAPHICAL ABSTRACT

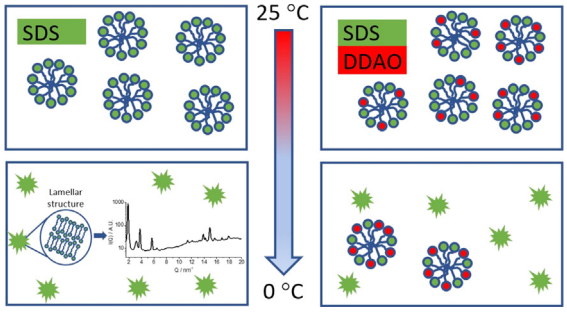

ARTICLE INFO

Article history:
Received 16 July 2018
Revised 12 September 2018
Accepted 15 September 2018
Available online 17 September 2018

Keywords:
Sodium dodecyl sulfate
N,N-dimethyldodecylamine N-oxide
Low temperature
Crystallization
Nuclear magnetic resonance
X-ray scattering

ABSTRACT

Surfactant crystallisation is important in many applications in the food, consumer product and medical sectors. However, these processes are not well understood. In particular, surfactant crystallisation can be detrimental to the stability of detergent formulations, such as dish liquid products, resulting in a turbid solution that fails appearance criteria. With the rising global demand for detergent products, understanding the factors that influence formulation stability is of increasing importance. To enable industry to build more robust formulations, it is important to understand the underlying chemistry of the crystallisation process. Here, a model system containing anionic (sodium dodecyl sulfate, SDS) and amphoteric (N,N-dimethyldodecylamine N-oxide, DDAO) surfactants, at concentrations typical of dish liquid products, is studied. Variable temperature ^{1}H nuclear magnetic resonance (NMR) spectroscopy and small-angle X-ray scattering (SAXS) is used to probe the compositional and structural properties of this system, as a function of pH. On cooling, at pH 9, a mixture of hydrated crystals, predominately composed of SDS, and micelles containing both surfactants, have been observed prior to complete freezing. At pH 2, both surfactants appear to undergo a simultaneous phase transition, resulting in the removal of micelles and the formation of hydrated crystals of mixed composition.

* Corresponding author.
E-mail address: m.m.britton@bham.ac.uk (M.M. Britton).

https://doi.org/10.1016/j.jcis.2018.09.053
0021-9797/

1. Introduction

Surfactants are important components in many applications, including the manufacture of food products, jet fuels, medical treatments and consumer products [1]. At low temperatures, such surfactants can crystallise, which may be either essential or detrimental to their performance in a given application [2]. Despite this importance, there remain relatively few studies on surfactant crystallisation, in particular the kinetics, crystal composition and structure. Of significant interest is surfactant crystallisation at low temperatures, which causes stability issues for liquid detergents. While this process is reversible, it is considered a failure in those products. Such failures can occur at any point during the product lifecycle, especially during transport and shelf-life stages. Hence, it is important to enhance the understanding of surfactant crystallisation in order to improve the stability of these formulations. Such knowledge will also be of significant interest in other applications of surfactants in food, biomedical and consumer product applications.

Common liquid detergents typically contain a mixture of anionic and amphoteric surfactants in an aqueous formulation [3] to optimise soil removal and foaming characteristics. Anionic surfactants are the major surfactant component and are cheap, efficient at removing soils and are largely responsible for the high foaming characteristics of the detergent [4]. The most commonly used anionic surfactant in liquid detergents is sodium dodecyl sulfate (SDS) [5]. While amphoteric surfactants comprise the minor surfactant component, they also play an important role by increasing the tolerance of the detergent to increased water hardness [6]. Common amphoteric surfactants found in liquid detergents are those based around the amine oxide functional group. One example of this is N, N-dimethyldodecylamine N-oxide (DDAO). At pH < 5, DDAO is protonated and behaves as a cationic surfactant, whereas at pH > 5 it is non-ionic [7,8]. In hand-dishwashing detergent products, commonly referred to as dish liquid, the typical pH is sufficiently high that amine oxide-based surfactants exhibit non-ionic surfactant-like behaviour.

In mixed micelles containing SDS and DDAO, the surfactant headgroups strongly interact, leading to a reduction in the critical micelle concentration, CMC, versus that of either surfactant alone [9]. Ion pairs form between the two surfactants which stabilise the mixed micelles through a shielding of the electrostatic repulsion between the SDS headgroups by those of DDAO [9]. Moreover, it is believed that the presence of SDS causes DDAO protonation to occur at a higher pH than that of pure DDAO [9,10]. Combining these surfactants is also expected to lower the Krafft temperature, T_K, in comparison to a pure SDS solution. This drop in T_K can be attributed to the lower CMC [11] of the system and the formation of non-ideal mixed micelles [12]. With DDAO present, there is expected to be a decrease in the concentration of SDS monomers and unbound counter-ions, and consequently a decreased tendency for precipitation.

Studies into the precipitation of mixed surfactant systems have been carried out to some extent, but there remains limited literature reporting the nature of the precipitate [6,13]. For example, HPLC was used to determine the composition of the precipitate formed when the non-ionic surfactant nonylphenol ethoxylate (NPE) was added to SDS and found that NPE was not present in the precipitate [6]. Furthermore, the composition of the precipitant from a bi-anionic surfactant system containing the surfactants SDS and sodium octylbenzene sulfonate (SOBS) has also been investigated via X-ray diffraction (XRD) [13]. In the mixed sample, two sets of peaks were observed with 2θ values corresponding to pure SDS and SOBS crystals, suggesting that mixed crystals were not formed. Aside from these studies, there are few reports regarding the composition of the precipitant formed from mixed surfactant systems below T_K.

Two techniques which can provide further compositional and structural insight into the crystallisation of mixed surfactant systems are temperature-resolved nuclear magnetic resonance (NMR) and small-angle X-ray scattering (SAXS). While there are few NMR studies of surfactant crystallisation from micelles, it has been used to follow the nucleation and freezing of individual components during the crystallisation of some emulsions [14] and food materials [15,16] by monitoring the change in individual NMR signals as a function of time. On the other hand, several studies have used SAXS or small-angle neutron scattering (SANS) to provide structural insight into various phase transitions [17–19], and to probe the structure and composition of micelles in dilute systems of both pure and mixed SDS and DDAO [20,21].

In this paper, NMR has been used to observe the crystallisation of a mixed micelle system, comprising SDS and DDAO surfactants, in water. NMR parameters for the two surfactants were monitored as the solution was cooled from 25 °C to −3 °C, at pH 9. By comparing the change in relative peak intensity for the two surfactants, it was possible to identify the crystal composition formed in this mixed micelle system. SAXS was used to probe the structure of the systems at room temperature and at 0 °C. Furthermore, a difference in the behaviour was observed upon lowing the pH of the system. By combining results from these complementary techniques, it has been possible to build a clearer picture of both the structure and composition of the phases that form in these systems under both pH environments.

2. Materials and methods

2.1. Materials

Surfactant solutions were prepared from DDAO (Sigma Aldrich, 30 wt.% in water) and SDS (Fisher Scientific, 97.5%) which were used without further purification. Binary surfactant solutions were prepared with 20 wt.% SDS and 3 wt.% DDAO in distilled water, for SAXS and WAXS measurements, and in D_2O (Sigma Aldrich, 99.9%), for NMR measurements. A correction was made to account for the density differences between D_2O and H_2O so that the molar surfactant concentration remained the same. A pure solution of 20 wt.% SDS solution was also prepared. Solutions were stirred for 15 min at ambient temperature and then left for 24 h. The pH of both the 20 wt.% SDS + 3 wt.% DDAO solution and 20 wt.% SDS solution were approximately pH 9. A second binary solution of 20 wt.% SDS + 3 wt.% DDAO solution was also prepared at pH 2 using a solution of 35 wt.% DCl in D_2O, for NMR measurements, or 0.5 M HCl in H_2O, for SAXS measurements. The pH was measured using a Meter Toledo pH meter.

2.2. Methods

2.2.1. Variable temperature NMR

NMR measurements were performed using Wilmad Precision 5 mm NMR tubes and a Bruker AVANCE NEO spectrometer equipped with a 11.74 T vertical bore magnet, operating at a ^1H resonance frequency of 500.07 MHz and fitted with a 5 mm nitrogen-cooled BBFO probe. Sample temperature was controlled using compressed air going through a chiller BCU-II unit and the probe heater. Samples were allowed to equilibrate at each temperature for a minimum of 15 min. Spectra at each temperature were acquired using a pulse acquire sequence, [90°-acq]. A spectral width of 15 kHz was used and 100 k complex data points were acquired. Sixteen signal averages were acquired with a repetition

time of 15 s. The repetition time used was greater than 5 T_1 for the protons in the SDS and DDAO surfactants. T_1 values are provided in the supplementary information (Table S2).

At pH 9, ^{1}H NMR spectra were acquired at the following temperatures: 25 °C, 20 °C, 15 °C, 13 °C, 10 °C, 5 °C, 0 °C and −3 °C. At pH 2, ^{1}H NMR spectra were acquired at 7.5 °C, 5 °C, 0 °C, −3 °C, −5 °C, −8 °C and −10 °C, corresponding to the range over which the phase transition occurs. Spectra were processed using TopSpin (v3.5). The NMR spectra for the individual SDS and DDAO systems, at pH 9, were acquired at 25 °C and the respective ^{1}H NMR signals assigned to the proton environments of the two surfactants (see supporting information Figs. S1 and S2 and Table S1). The H_1 (SDS) peak was set at 3.7 ppm at 25 °C, determined from SDS [22] in DMSO d_6, and remaining spectra were adjusted with respect to this. The NMR signals for the SDS and DDAO surfactants were determined using the peak intensities for the H_1 and H_a protons, respectively. Each peak was normalised with respect to its intensity at 25 °C, to enable the direct comparison of the changes between the peaks to be made. Peak intensities are used, rather than integrals, to enable the observation of changes in molecular mobility through its effects on the line width, and hence intensity, as well as avoiding unwanted influences from overlapping, but unrelated, peaks (an effect which increases as the peaks become broader at lower temperatures). Error bars were determined from repeated measurements.

2.2.2. Small angle X-ray scattering

Small angle scattering (SAXS) data was obtained using the I22 beamline at Diamond Light Source. Samples were loaded into 1.8 mm (internal diameter) and 2.0 mm (external diameter) polycarbonate capillaries and mounted in the beam within the Linkam DSC600 capillary stage, which also provided temperature control (at 24 °C and 0 °C, with an applied cooling rate = 19 °C/min). A 12.3989 keV (λ = 0.099987 nm) beam was used with a sample-detector distance of 6702.56 mm, providing a detectable *Q*-range on the SAXS detector of order 0.02–2.5 nm^{-1} and 1.51–60.57 nm^{-1} on the WAXS detector. Data processing was performed using the DAWN package [23,24], and a set of pipelines developed at Diamond Light Source. Before processing, uncertainty estimates based on Poisson counting statistics are added to all measurement data, which are subsequently propagated through the image correction steps. Each raw background measurement was corrected for the following in order: masking pixels, time, incident beam flux, and transmission. Each sample file was corrected for the following in order: masking pixels, time, incident beam flux, transmission, background, thickness, and scaled to absolute units. The scaling factor for scaling to absolute units was determined using a calibrated glassy carbon sample [25]. After this correction, the data was azimuthally averaged, with the resulting uncertainty assuming the largest of: (1) the propagated uncertainties, (2) the standard error of the mean for the data points comprising a bin, or (3) 1% of the mean intensity in the bin.

The data at 24 °C was analysed using the SASfit software package [26]. There is some discussion in the literature concerning whether SDS micelles are oblate or prolate ellipsoids [20,21,27–29]. The two options are difficult to distinguish using scattering techniques, but the prolate model is considered to be more appropriate in denser systems [28]. Several small-angle scattering studies, including one that focused on mixed micelles comprising SDS and DDAO [20], have favoured the prolate shape. Consequently, a model comprising a delta distribution of charged core-shell prolate ellipsoids, as outlined in the supporting information, was used to analyse the data. A breakdown of the *S(Q)* and *P(Q)* contributions to the overall fit is shown in Fig. S3 and the analysis parameters are provided in Table S3.

The data at 0 °C for both the pure SDS solution and the mixed SDS + DDAO system was also analysed using SASfit,[26] in both cases using a simple model comprising contributions from one or more Bragg peak(s), the power law and the background scattering (see details in SI). For the 20 wt.% SDS + 3 wt.% DDAO sample, an additional contribution of delta distribution of charged core–shell prolate ellipsoids was added, to account for the increased *I(Q)* at high *Q*.

3. Results and discussion

Fig. 1 displays a series of ^{1}H NMR spectra acquired from 25 °C to −3 °C, with an expansion of the region between 2.6 and 4.0 ppm, for the mixed SDS + DDAO system at pH 9. The change in peak

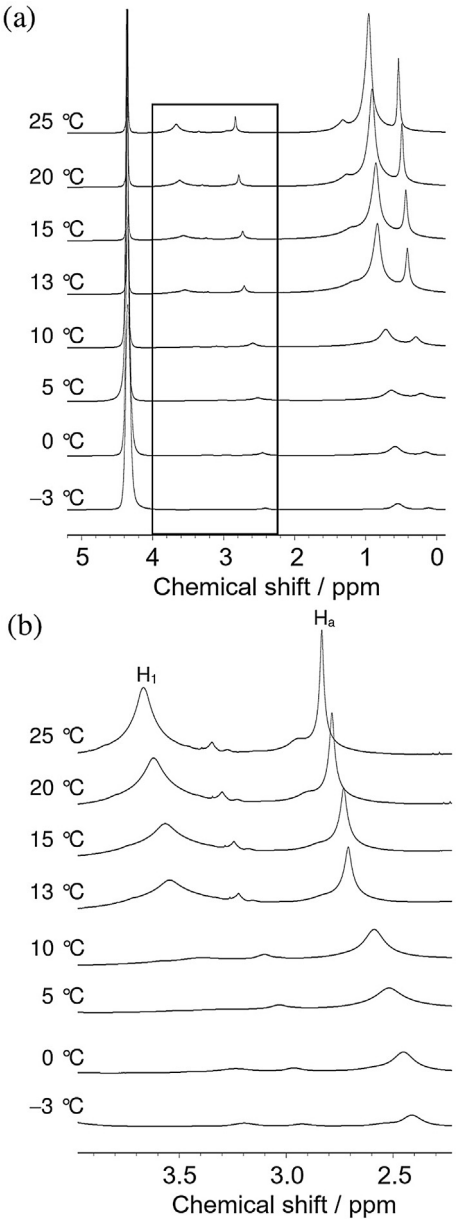

Fig. 1. ^{1}H NMR spectra at 500 MHz of the 20 wt.% SDS + 3 wt.% DDAO system upon cooling at pH 9 across the chemical shift range (a) 0–5 ppm and (b) 2.3–4.0 ppm. The boxed area in (a) corresponds to the chemical shift range presented in (b). Proton resonance H_1 (SDS) is at 3.67 ppm and H_a (DDAO) is at 2.83 ppm. A full spectral assignment can be found in the SI.

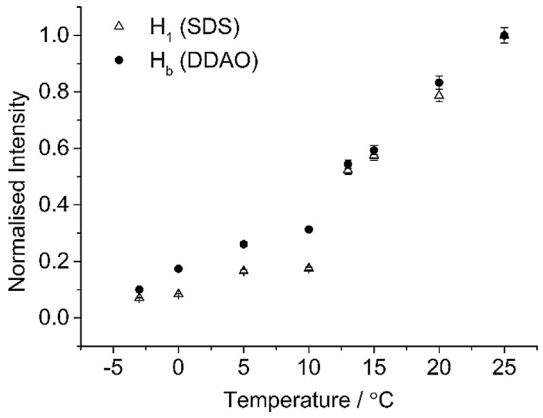

Fig. 2. Plot of the peak intensity for H_1 (SDS) and H_a (DDAO) upon cooling at pH 9. Each peak has been normalised, with respect to the intensity of that peak at 25 °C, and includes a slight baseline offset.

intensity as a function of temperature for the protons H_1 (SDS) and H_a (DDAO) under this pH environment is presented in Fig. 2. At pH 9, there is a significant drop in the peak intensity of the ^{1}H NMR signal of H_1 (SDS) between 10 °C and 13 °C. A similar trend is not observed for H_a in DDAO. Although the peak intensity of the H_a (DDAO) also exhibits a reduction in peak intensity, the drop between 10 °C and 13 °C is not as significant as H_1 (SDS). Instead, the intensity decreases at a consistent rate.

In contrast, at pH 2, both surfactants display a sharp drop intensity between −5 °C and −3 °C (Fig. 3). There is a change in the chemical shifts for the H_a (DDAO) peak, compared to the H_1 (SDS) peak at pH 2, because of the change in environment experienced by these protons when the headgroup is protonated.[30–32] In addition, at pH 2, there are a greater number of peaks in the region of interest, attributed to an interaction between the two charged surfactant species resulting in further proton environments.

In Fig. 4, the SAXS profiles, at 24 °C and 0 °C, for the mixed system are compared to the corresponding profiles for a pure SDS system. In Fig. 4(a), a cropped Q-range is shown due to the high error in the low Q (<0.8 nm^{-1}) part of the data arising from the weak sample scattering versus background compounded by a high sample volume fraction. The data, collected at 24 °C, is characterised by two merged maxima resulting from a form factor, $P(Q)$ corresponding to the electron-dense micelle shell and a structure factor, $S(Q)$ arising from the micelle charge. The addition of DDAO causes a shift in the low Q maxima to a lower Q. Cooling both samples to 0 °C results in a notable change in the SAXS data, shown in Fig. 4 (b). For the 20 wt.% SDS sample, an increase in $I(Q)$ at low Q is observed followed by a region over which $I(Q) \propto Q^{-4}$ and a Bragg peak at $Q = 1.9$ nm^{-1} The 20 wt.% SDS + 3 wt.% DDAO data at 0 °C is similar to that for the pure SDS sample, except for an increased $I(Q)$ in the region $0.7 < Q < 2.5$ nm^{-1}, which has a similar shape to that presented in Fig. 4(a).

At pH 2, the profile acquired at 0 °C exhibits two Bragg peaks (Fig. 5) with neither peak matching the Bragg peak previously observed (Fig. (4b)) in the pure SDS and mixed SDS + DDAO systems at pH 9. The corresponding peak shift values for the three systems (20 wt.% SDS, 20 wt.% SDS + DDAO (pH 9) and 20 wt.% + 3 wt.% DDAO (pH 2)) at 0 °C are provided in the supplementary information. Further comparisons regarding the crystal structure can also be drawn from the WAXS for the three different systems, as depicted in Fig. 6.

At pH 9, the ^{1}H NMR data suggests that SDS crystallises first, before the system fully solidifies. The drop in NMR signal for the SDS and DDAO protons is expected to be associated with an

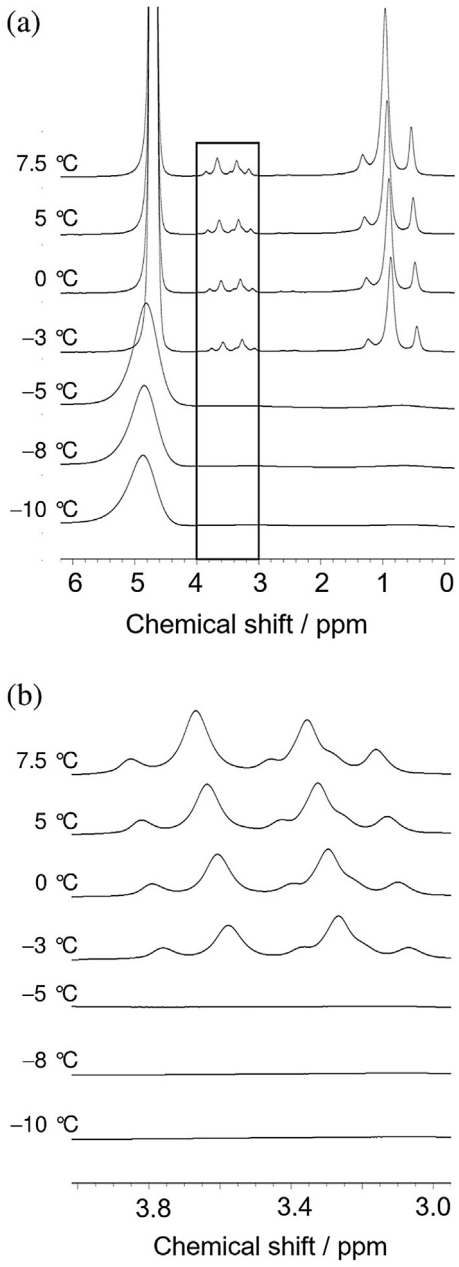

Fig. 3. ^{1}H NMR spectra at 500 MHz of the 20 wt.% SDS + 3 wt.% DDAO system upon cooling at pH 2 across the chemical shift range (a) 0–6 ppm and (b) 3.0–4.0 ppm. The boxed area in (a) corresponds to the chemical shift range presented in (b). Proton resonance H_1 (SDS) is at 3.67 ppm and H_a (DDAO) is at 3.35 ppm.

increase in viscosity and a reduction in the mobility of the monomers and micelles, leading to a reduction in their T_2^* NMR relaxation time and an increase in the width of their peaks [33]. There is a sudden drop in SDS signal between 10 °C and 13 °C, which indicates SDS is undergoing a phase transition. However, not all of the SDS signal disappears at the lower temperature, indicating a proportion of the SDS remains in solution. The DDAO does not display a sudden drop in the signal, suggesting it is not residing in the crystal itself, yet, there is a decrease indicating that the DDAO surfactant is affected by the SDS crystal formation between 10 °C and 13 °C. In a previous study, confocal Raman microscopy indicated a tendency for DDAO to surround the SDS hydrated crystals and, therefore, is influenced

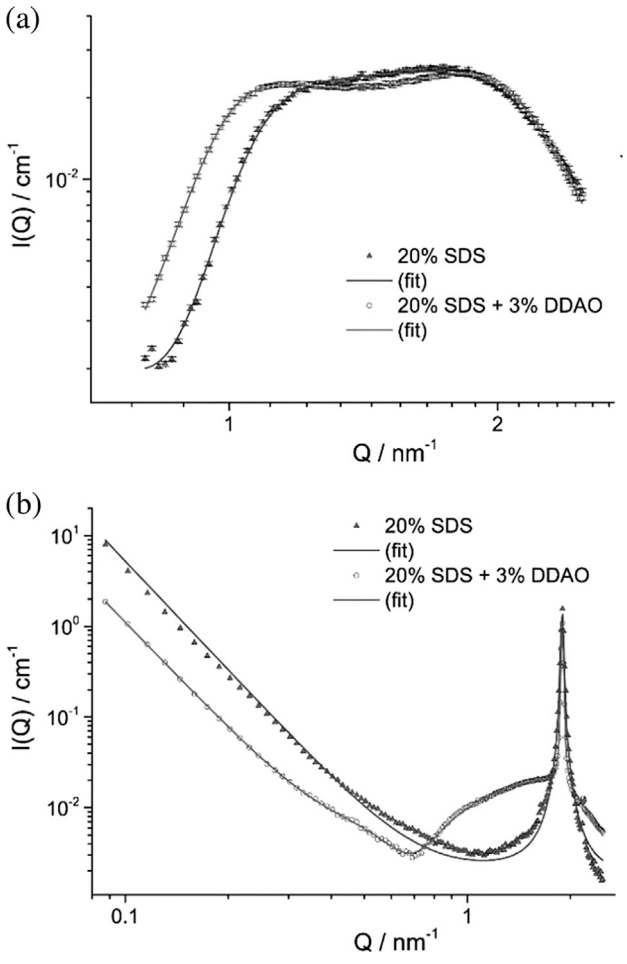

Fig. 4. SAXS data for 20 wt.% SDS and 20 wt.% SDS + 3 wt.% DDAO samples at **(a)** 24 °C and **(b)** 0 °C. In both cases, the solid lines are fits to the data as described in the text and supplementary information.

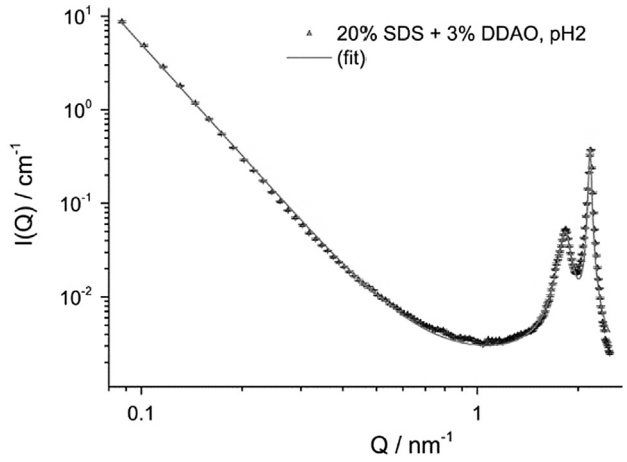

Fig. 5. SAXS data for 20 wt.% SDS and 20 wt.% SDS + 3 wt.% DDAO samples at pH 2. The solid lines are fits to the data as described in the text and supplementary information.

by their formation, which potentially explains the decrease in the DDAO signal [34].

SAXS data at 24 °C suggests that pure SDS micelles and mixed SDS + DDAO micelles co-exist in the system. The differences between profiles obtained for a pure SDS and a mixed SDS + DDAO

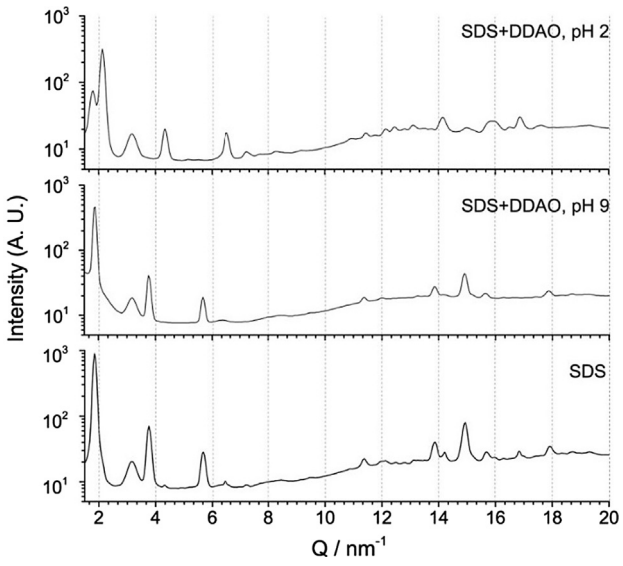

Fig. 6. WAXS data for the three samples as noted at 0 °C. Concentrations of SDS and DDAO, where present, are 20 wt.% and 3 wt.% respectively. The peak at 3.15 nm^{-1} is from the polycarbonate capillary used to mount samples in the beam. All other peaks arise from the samples. From these, significant peaks are listed in Table S5 (supplementary).

system indicate there is an increase in micelle size when DDAO is present, which is in line with previous observations [20]. By adding 3 wt.% DDAO, to a solution of SDS, the micelle aggregation number, N_{agg}, increases from 170 to 190 and the ellipsoid aspect ratio, a/b, from 1.8 to 2.2. Conversely, the proportional charge per headgroup, Z/N_{agg} falls from 0.12 to 0.11. This reduction in charge is in agreement with the literature [20], and is expected to reduce repulsions between the SDS head-groups in the interphase. Consequently, the shell curvature is able to decrease, allowing a more elongated structure to form.

The formation of a Bragg peak in the pure SDS system at 0 °C indicates the growth of SDS crystallites [21]. The calculated d-spacing, $d = 3.3$ nm, is closer to the values expected for the mono- or hemi-hydrated crystal forms (2.9 or 3.1 nm respectively), but lower than that of the 1/8 hydrate (3.9 nm) [35]. For the mixed SDS + DDAO system, the Bragg peak position is the same as the pure SDS system, indicating SDS is the dominant component of the crystals in both samples. This is in agreement with the drop in intensity of NMR signal observed for the SDS protons (H_1) (Fig. 2). Aside from the Bragg peak, there is an additional contribution in the SAXS profile for the mixed system, which can be fitted to the remaining micelle phase. For the remaining micelles, $N_{agg} = 240$ and $a/b = 2.4$, which is more in line with data reported for mixed SDS + DDAO micelles than that for DDAO micelles alone [20]. Moreover, the micelles remain charged, albeit with a lower Z/N_{agg} than the values reported at 24 °C. Put together, the scattering data and associated analysis provides compelling evidence that the crystallites formed in the mixed SDS + DDAO system contain predominantly SDS, in agreement with NMR data. Unlike in the pure SDS system, not all SDS crystallises and some remains within a mixed micelle population, as is also observed in the NMR data. Thus, the remaining NMR signal originates from micelles containing DDAO and SDS. By adding DDAO, the energy to form micelles is reduced, consequently diminishing the energetic driving force for crystallisation, consequently leading to a shift in the equilibrium towards micelles remaining in solution.

At pH 2, both SAXS and NMR studies suggest a simultaneous change in the phase behaviour of each surfactant. The NMR data shows the SDS and DDAO surfactants crystallise at the same time.

This observation is expected to be because of the formation of the protonated form of DDAO, which can ion pair with SDS and counter-ions [9,36]. This is further supported by peaks at differing shifts in the corresponding SAXS profile, compared to that of the pure SDS and the mixed pH 9 system.

Further detail into the structure of the SDS crystallites can be drawn from WAXS data (Fig. 6), with comparisons for notable peaks given in Table S5 (supplementary). After holding at 0 °C for 45 min, at pH 9, the peaks in the mixed system can be matched, within error, to those observed in the pure SDS system, further indicating the formation of the same SDS phase. Peaks at 1.87, 3.76, 5.68 and 11.35 nm^{-1} are assigned as first, second, third and sixth-order lamellar *d*-spacings (d = 3.34 nm) while peaks at higher *Q* (*e.g.* at 13.9, 14.9, 15.6 and 17.9 nm^{-1}) may arise from the head-head and alkyl peaks.[37] In the pure SDS system, more peaks are apparent in this region. However, as the peak intensities for this sample are approximately 2–3 times more intense, over the entire *Q*-range, this is more likely to be an observational artefact arising from a low peak intensity versus background. In contrast, at pH 2, a different structure forms, with first, second and third order lamellar d-spacings shifted to higher *Q* (at 2.13, 4.33 and 6.52 nm^{-1} respectively) giving d = 2.95 nm. This suggests the formation of crystals containing both surfactants.

4. Conclusions

By combining variable temperature ^{1}H NMR and SAXS measurements it has been possible, for the first time, to determine the compositional and structural changes in a mixed SDS and DDAO surfactant system, which is of particular interest in the fast moving consumer goods (FMCG) industry [38]. Crystals formed as the mixed SDS + DDAO system is cooled, at pH 9, are observed to be predominately SDS hydrated crystals, with little or no DDAO. At pH 2, the protonated DDAO, and its subsequent ion pairing behaviour, results in both surfactants crystallising simultaneously. While dish liquid is a highly complex system, this research provides important insight into the crystallisation process of liquid detergent systems upon exposure to cold climates. In turn, this understanding will assist in building more robust formulations and improvements to their accompanying test methods.

Associated content

The following files are available free of charge.
NMR spectral assignments and the SAXS model fitting (PDF)

Acknowledgments

We would like to gratefully acknowledge the Engineering and Physical Sciences Council for their financial support (Grant Reference EP/G036713/1). Thanks also go to the facilities at the Diamond Light Source that enabled the SAXS data to be acquired.

Appendix A. Supplementary material

Supplementary data to this article can be found online at https://doi.org/10.1016/j.jcis.2018.09.053.

References

[1] J.-L. Salager, Surfactants types and uses, FIRP booklet 2002.
[2] E. Summerton, G. Zimbitas, M. Britton, S. Bakalis, Low temperature stability of surfactant systems, Trends Food Sci. Technol. 60 (2017) 23–30.
[3] G. Kume, M. Gallotti, G. Nunes, Review on anionic/cationic surfactant mixtures, J. Surfactants Deterg. 11 (2008) 1–11.
[4] K. Holmberg, B. Jönsson, B. Kronberg, B. Lindman, Surfactants and Polymers in Aqueous Solution, Wiley Online Library, 2003.
[5] M. Dierker, H.J. Schafer, Surfactants from oleic, erucic and petroselinic acid: synthesis and properties, Eur. J. Lipid Sci. Technol. 112 (2010) 122–136.
[6] K.L. Stellner, J.F. Scamehorn, Hardness tolerance of anionic surfactant solutions. 2. Effect of added nonionic surfactant, Langmuir 5 (1989) 77–84.
[7] J.F. Rathman, S.D. Christian, Determination of surfactant activities in micellar solutions of dimethyldodecylamine oxide, Langmuir 6 (1990) 391–395.
[8] K.W. Herrmann, Non-ionic-cationic micellar properties of dimethyldodecylamine oxide, J. Phys. Chem. 66 (1962) 295–300.
[9] T.P. Goloub, R.J. Pugh, B.V. Zhmud, Micellar interactions in nonionic/ionic mixed surfactant systems, J. Colloid Interf. Sci. 229 (2000) 72–81.
[10] S. Soontravanich, J.A. Munoz, J.F. Scamehorn, J.H. Harwell, D.A. Sabatini, Interaction between an anionic and an amphoteric surfactant. Part I: Monomer-Micelle Equilibrium, J. Surfactants Deterg. 11 (2008) 251–261.
[11] X.J. Fan, P. Stenius, N. Kallay, E. Matijevic, Precipitation of surfactant salts. 2. The effect of nonionic surfactants on precipitation of calcium dodecyl-sulfate, J. Colloid Interf. Sci. 121 (1988) 571–578.
[12] J.F. Scamehorn, An overview of phenomena involving surfactant mixtures, ACS Symp. Ser. 311 (1986) 1–27.
[13] S. Soontravanich, Formation and Dissolution of Surfactant Precipitates, University of Oklahoma, 2007.
[14] J.P. Hindmarsh, K.G. Hollingsworth, D.I. Wilson, M.L. Johns, An NMR study of the freezing of emulsion-containing drops, J. Colloid Interf. Sci. 275 (2004) 165–171.
[15] A. Gallo, M.F. Mazzobre, M.P. Buera, M.L. Herrera, Low resolution ^{1}H-Pulsed NMR for sugar crystallization studies, Lat. Am. Appl. Res. 33 (2003) 97–102.
[16] J. Kolz, Y. Yarovoy, J. Mitchell, M.L. Johns, L.F. Gladden, Interactions of binary liquid mixtures with polysaccharides studied using multi-dimensional NMR relaxation time measurements, Polymer 51 (2010) 4103–4109.
[17] M.J. Hollamby, Practical applications of small-angle neutron scattering, Phys. Chem. Chem. Phys. 15 (2013) 10566–10579.
[18] R.F. Tabor, J. Eastoe, I. Grillo, Time-resolved small-angle neutron scattering as a lamellar phase evolves into a microemulsion, Soft Matter 5 (2009) 2125–2129.
[19] F.-G. Wu, N.-N. Wang, J.-S. Yu, J.-J. Luo, Z.-W. Yu, Nonsynchronicity Phenomenon Observed during the Lamellar– Micellar Phase Transitions of 1-Stearoyllysophosphatidylcholine Dispersed in Water, J. Phys. Chem. B 114 (2010) 2158–2164.
[20] M. Kakitani, T. Imae, M. Furusaka, Investigation of mixed micelles of dodecyldimethylamine oxide and sodium dodecyl sulfate by SANS: shape, size, charge, and interaction, J. Phys. Chem. 99 (1995) 16018–16023.
[21] B. Hammouda, Temperature effect on the nanostructure of SDS micelles in Water, J. Res. Natl. Inst. Stand. Technol. 118 (2013) 151–167.
[22] Spectral database for organic compounds SDBS. Available at <http://sdbs.db.aist.go.jp/sdbs/cgi-bin/direct_frame_top.cgi> Accessed (13/06/2018).
[23] J.F. van der Veen, JSR - XFELs, DLSRs and beamline articles, J. Synchrotron Rad. 22 (2015) 1–2.
[24] J. Filik, A.W. Ashton, P.C.Y. Chang, P.A. Chater, S.J. Day, M. Drakopoulos, M.W. Gerring, M.L. Hart, O.V. Magdysyuk, S. Michalik, A. Smith, C.C. Tang, N.J. Terrill, M.T. Wharmby, H. Wilhelm, Processing two-dimensional X-ray diffraction and small-angle scattering data in DAWN 2, J. Appl. Crystallogr. 50 (2017) 959–966.
[25] F. Zhang, J. Ilavsky, G.G. Long, J.P.G. Quintana, A.J. Allen, P.R. Jemian, Glassy carbon as an absolute intensity calibration standard for small-angle scattering, Metall. Mater. Trans. A 41 (2010) 1151–1158.
[26] I. Bressler, J. Kohlbrecher, A.F. Thunemann, SASfit: a tool for small-angle scattering data analysis using a library of analytical expressions, J. Appl. Crystallogr. 48 (2015) 1587–1598.
[27] M. Bergstrom, J. Skov Pedersen, Structure of pure SDS and DTAB micelles in brine determined by small-angle neutron scattering (SANS), Phys. Chem. Chem. Phys. 1 (1999) 4437–4446.
[28] S. Vass, J.S. Pedersen, J. Pleštil, P. Laggner, E. Rétfalvi, I. Varga, T. Gilányi, Ambiguity in determining the shape of alkali alkyl sulfate micelles from small-angle scattering data, Langmuir 24 (2008) 408–417.
[29] G. Garg, P.A. Hassan, V.K. Aswal, S.K. Kulshreshtha, Tuning the structure of SDS micelles by substituted anilinium ions, J. Phys. Chem. B 109 (2005) 1340–1346.
[30] R. Vijay, J. Singh, G. Baskar, R. Ranganathan, Amphiphilic lauryl ester derivatives from aromatic amino acids: significance of chemical architecture in aqueous aggregation properties, J. Phys. Chem. B 113 (2009) 13959–13970.
[31] V.G. Gaikar, K.V. Padalkar, V.K. Aswal, Characterization of mixed micelles of structural isomers of sodium butyl benzene sulfonate and sodium dodecyl sulfate by SANS, FTIR spectroscopy and NMR spectroscopy, J. Mol. Liq. 138 (2008) 155–167.
[32] M. Bhat, V.G. Gaikar, Characterization of interaction between butyl benzene sulfonates and cetyl trimethylammonium bromide in mixed aggregate systems, Langmuir 15 (1999) 4740–4751.
[33] T.L. James, Fundamentals of NMR. Online Textbook: Department of Pharmaceutical Chemistry, University of California, San Francisco, 1998, pp. 1–31.
[34] E. Summerton, M.J. Hollamby, G. Zimbitas, T. Snow, A.J. Smith, J. Sommertune, J. Bettiol, C. Jones, M.M. Britton, S. Bakalis, The impact of N, N-dimethyldodecylamine N-oxide (DDAO) concentration on the crystallisation of sodium dodecyl sulfate (SDS) systems and the resulting changes to crystal structure, shape and the kinetics of crystal growth, J. Colloid Interf. Sci. 527 (2018) 260–266.

[35] R.M. Miller, A.S. Poulos, E.S.J. Robles, N.J. Brooks, O. Ces, J.T. Cabral, Isothermal crystallization kinetics of sodium dodecyl sulfate-water micellar solutions, Cryst. Growth Des. 16 (2016) 3379–3388.
[36] A. Búcsi, J. Karlovská, M. Chovan, F. Devínsky, D. Uhríková, Determination of pKa of N-alkyl-N, N-dimethylamine-N-oxides using ^{1}H NMR and ^{13}C NMR spectroscopy, Chem. Pap. 68 (2014) 842–846.
[37] S.T. Hyde, Identification of Lyotropic Liquid Crystalline Mesophases, Handbook of Applied Surface & Colliod Chemistry, John Wiley & Sons, Ltd., 2001.
[38] E. Summerton, G. Zimbitas, M. Britton, S. Bakalis, Crystallisation of sodium dodecyl sulfate and the corresponding effect of 1-dodecanol addition, J. Cryst. Growth 455 (2016) 111–116.